ISSN 1063-7745, Crystallography Reports, 2015, Vol. 60, No. 4, pp. 565–569. © Pleiades Publishing, Inc., 2015.
Original Russian Text © A.V. Butashin, V.M. Kanevsky, A.E. Muslimov, P.A. Prosekov, O.A. Kondratev, A.E. Blagov, A.L. Vasil'ev, E.V. Rakova, V.A. Babaev, A.M. Ismailov, E.A. Vovk, S.V. Nizhankovsky, 2015, published in Kristallografiya, 2015, Vol. 60, No. 4, pp. 620–624.

SURFACE AND THIN FILMS

Growth of Crystalline ZnO Films on the Nitridated (0001) Sapphire Surface

A. V. Butashin[a], V. M. Kanevsky[a], A. E. Muslimov[a], P. A. Prosekov[a, d], O. A. Kondratev[a, d], A. E. Blagov[a, d], A. L. Vasil'ev[a, d], E. V. Rakova[a], V. A. Babaev[b], A. M. Ismailov[b], E. A. Vovk[c], and S. V. Nizhankovsky[c]

[a] *Shubnikov Institute of Crystallography, Russian Academy of Sciences, Moscow, 119333 Russia*
[b] *Dagestan State University, Makhachkala, 367000 Russia*
[c] *Institute for Single Crystals, National Academy of Sciences of Ukraine, Kharkov, 61103 Ukraine*
[d] *National Research Centre "Kurchatov Institute", pl. Akademika Kurchatova 1, Moscow, 123182 Russia*
e-mail: amuslimov@mail.ru

Received January 22, 2015

Abstract—The surface morphology and structure of (0001) sapphire substrates subjected to thermochemical nitridation in a mixture of N_2, CO, and H_2 gases are investigated by electron and probe microscopy and X-ray and electron diffraction. It is shown that an aluminum nitride layer is formed on the substrate surface and heteroepitaxial ZnO films deposited onto such substrates by magnetron sputtering have a higher quality when compared with films grown on sapphire.

DOI: 10.1134/S1063774515040094

INTRODUCTION

Crystalline films of wide-gap semiconductor ZnO are of great interest for application in piezoelectric engineering, optoelectronics, and photonics. These films are fabricated by molecular beam epitaxy (MBE), laser ablation, and magnetron sputtering [1–6]. Epitaxy of these films is often performed on (0001) α-Al_2O_3 sapphire plates, despite the significant lattice mismatch of the film and substrate. However, the thus grown heteroepitaxial ZnO films contain twins and domains with different orientations of polar axes; in addition, the film surface is characterized by enhanced roughness [1, 3, 4].

High-temperature annealing of Al_2O_3 (0001) substrates in air leads to the formation of regular nanostructures in the form of parallel terraces and steps on their surface and facilitates the suppression of twins and domains in the ZnO films prepared by magnetron sputtering [5, 6]. It was noted that the structural quality of MBE-grown ZnO films is significantly increased when the sapphire substrate surface is nitridated in an ionized nitrogen flux with the formation of a thin (up to 3 nm) aluminum nitride layer before growing ZnO [2].

In this study we comprehensively characterize the surface of (0001) sapphire substrates subjected to thermochemical nitridation and investigate the effect of the latter on the morphology and structure of heteroepitaxial ZnO films obtained by magnetron sputtering.

EXPERIMENTAL

Samples were Al_2O_3 plates 50.8 mm in diameter with a thickness of 0.43 mm subjected to chemical mechanical polishing. The thermochemical nitridation of the substrates was performed at a temperature of 1450°C in a mixture of N_2, CO, and H_2 gases (pressure 0.1–0.12 MPa, nitrogen concentration N_2 ~ 99 vol %), using the technique described in detail in [10]. The reduction potential of the annealing medium was controlled by varying the CO_2/CO and H_2O/H_2 ratio.

ZnO was deposited onto nitridated sapphire substrates in a magnetron sputtering chamber, where they were heated to a temperature of 650°C in an oxygen atmosphere at a pressure of 1.33 Pa under direct current (current density j = 10–60 mA cm^{-2}, film growth rate of ~2 nm s^{-1}). The magnetron sputtering technique we used was described in detail in [11]. The films grown had a thickness of about 200 nm.

The phase composition and orientation of the films were determined by reflection high-energy electron diffraction (RHEED) on an EMR-102 electronograph (accelerating voltage 75 kV).

The surface morphology of the sapphire substrates and grown ZnO films was studied on an Ntegra Aura

atomic force microscope in the topography mode. The microstructure and chemical composition of the layers on the sapphire substrate surface after nitridation were investigated in more detail by transmission electron microscopy (TEM) and scanning transmission electron microscopy (STEM). Specimens of nitridated layer/Al_2O_3 substrate transverse cuts for TEM/STEM studies were prepared using a focused Ga^+ ion beam in a Helios electron-ion scanning microscope (FEI, United States) using a standard technique. Before the procedure, a (0.5–1)-μm-thick Pt film was deposited onto the sapphire substrate using a gas injection system. The Ga^+ ion energy was 30 kV in the beginning and 2 kV at the end of the process. The transverse cuts were investigated on a Titan 80-300 microscope (FEI) equipped with a spherical aberration corrector, high-angle annular dark field detector (HAADF, Fischione, United States), and an energy-dispersive X-ray microanalysis system (EDAX, United States) at a voltage of 300 kV.

X-ray diffraction studies were carried out on an automated SmartLab Rigaku diffractometer (9 kW) equipped with an X-ray source having a rotating copper anode (λ = 1.540562 Å). The measurements were performed using a standard two-crystal diffractometry scheme in horizontal reflection geometry. Radiation was collimated by a Ge (220) symmetric double monochromator and then limited in the diffraction plane by a slit located in front of the sample and two slits mounted in front of a scintillation NaI detector. The potential of the X-ray optical scheme we used was described in more detail in [12]. This equipment and techniques were successfully used to study heteroepitaxial layers [13] up to 100 nm thick.

Rocking curves of the epitaxial ZnO layers were measured on two samples (with a ~200-nm-thick AlN layer and without it). The rocking curves were recorded in the (θ–2θ)-scan scheme. Spatial resolution in the diffraction plane was 0.5 mm; the receiving slits in front of the detector ensured an angular resolution $\Delta\theta_d$ = 0.025° for detecting the diffraction component on the reflected spectrum.

RESULTS AND DISCUSSION

According to the electron microscopy data on the AlN/Al_2O_3 transverse cut (Fig. 1), thermochemical nitridation led to the formation of a continuous alumi-

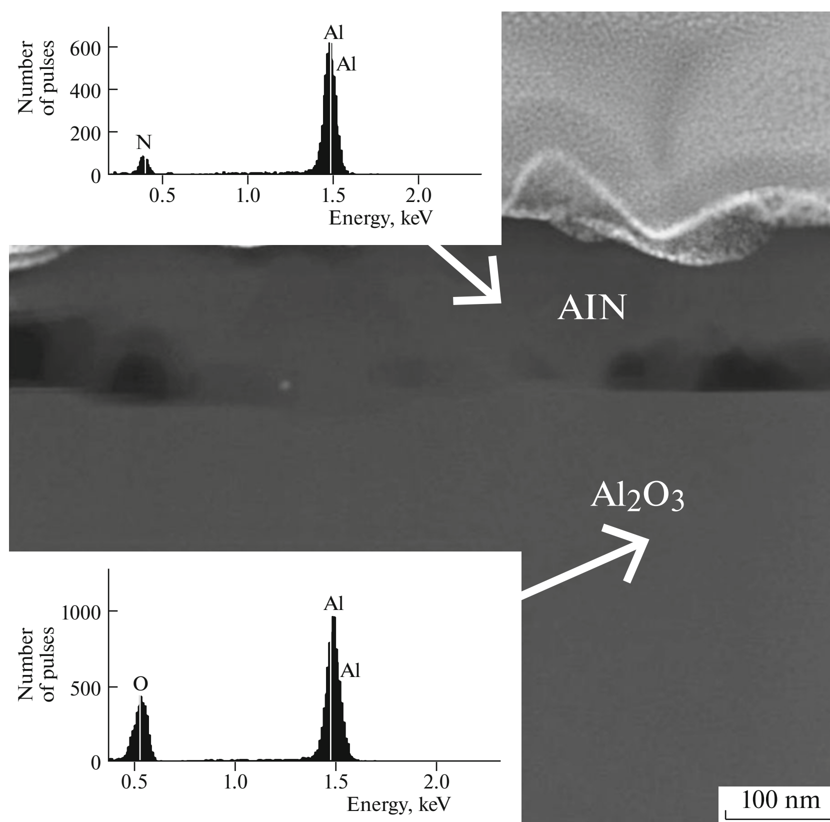

Fig. 1. STEM image (obtained with a HAADF detector) of a transverse cut of sapphire substrate surface after thermochemical nitridation and SEM data from different depths of the heterosystem (insets).

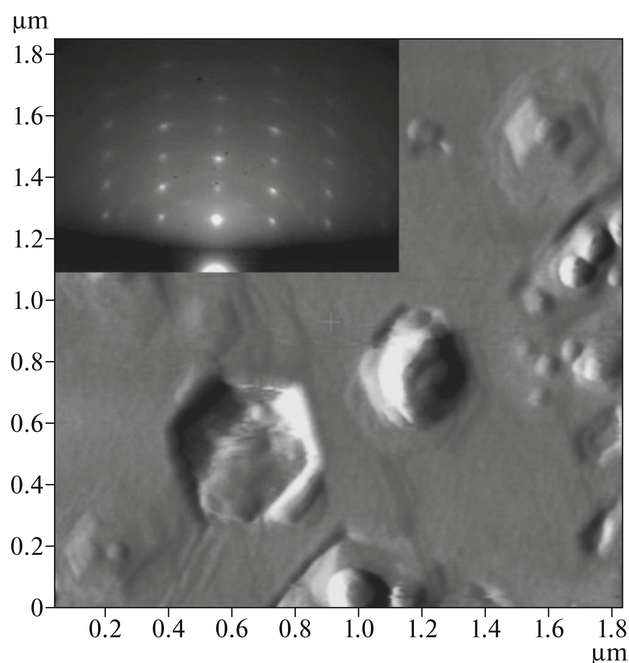

Fig. 2. AFM image (contact scanning mode) of the (0001) surface of a sapphire substrate after thermochemical nitridation and the corresponding electron diffraction pattern (inset).

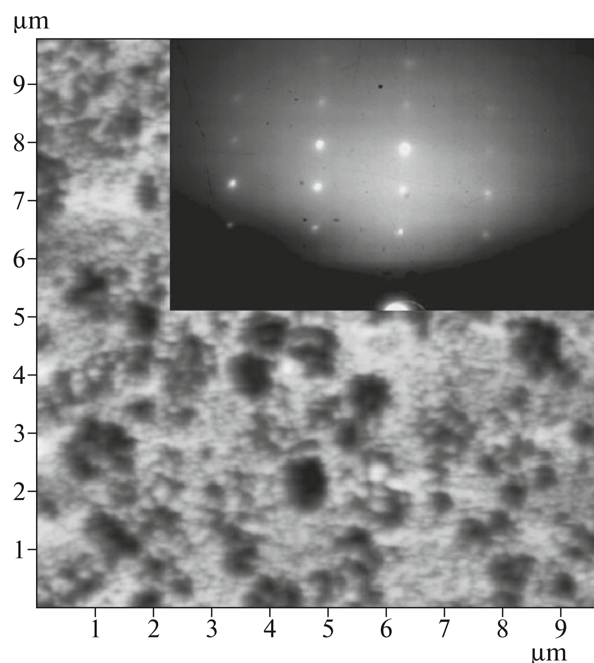

Fig. 3. AFM image of a zinc oxide film on a (0001) sapphire substrate with nitridated surface and the corresponding electron diffraction pattern (inset).

num nitride film with a thickness of 100 nm on the sapphire substrate surface with a sharp AlN/Al_2O_3 interface between the layer and substrate. The scanning electron microscopy data confirm the complete nitridation of the surface layer of the leucosapphire substrate to a depth of ~100 nm.

According to the RHEED data, the single-crystal AlN phase with a hexagonal wurtzite-type structure is formed on the sapphire substrate surface subjected to thermochemical nitridation (Fig. 2, inset). Indexing of the electron diffraction pattern shows that the (0001) plane of the AlN layer is oriented parallel to the substrate surface and consists of slightly misoriented blocks. It can be seen that the nitride film surface contains characteristic hexagonal etching pits with a linear edge size of up to 200 nm and a depth of up to 10 nm (Fig. 2). Such formations increase the substrate surface roughness to 4–5 nm.

The surface of the ZnO films grown on nitridated Al_2O_3 substrates had a granular microstructure with a grain size of 50–70 nm (Fig. 3). The surface contained craters with a linear size of up to 1 μm and a depth of up to 50 nm, which were probably formed on substrate surface defects. An analysis of the corresponding electron diffraction pattern (Fig. 3, inset) shows that the ZnO films crystallize in the wurtzite phase and their (0001) plane is oriented parallel to the (0001) AlN plane. There are no additional reflections indicative of the presence of domains or twins.

Electron diffraction patterns of the epitaxial ZnO films on the sapphire substrates subjected to chemical mechanical polishing without thermochemical nitridation contain additional reflections and rings (Fig. 4) which indicate the formation of domains and twins in the ZnO film and the presence of misoriented crystallites.

Figure 5 shows experimental rocking curves from the (002) planes of epitaxial ZnO films for two structures, ZnO/Al_2O_3 and $ZnO/AlN/Al_2O_3$. A comparison of the curves shows that the intensity of reflection from the ZnO (002) plane for the $ZnO/AlN/Al_2O_3$ structure is much higher (by a factor of 800) and the curve half-width is much smaller (by a factor of 7) than for ZnO/Al_2O_3. As well as RHEED patterns, the X-ray

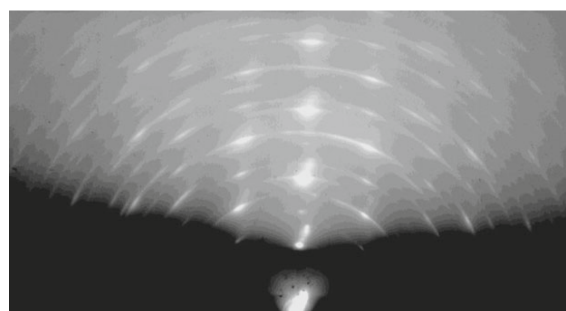

Fig. 4. Electron diffraction pattern of a zinc oxide film on a (0001) sapphire substrate after chemical mechanical polishing without nitridation.

Structural data for the crystals investigated

Composition	Structural type	sp. gr.	Lattice parameters *a* and *c*, nm	*Z*	Reference
Al_2O_3	corundum	$R\bar{3}c$	0.47540 (5), 1.29820 (6)	6	[7]
AlN	wurtzite	$P6_3mc$	0.3112, 0.4982	2	[8]
ZnO	wurtzite	$P6_3mc$	0.3249 (6), 0.52042 (20)	2	[9]

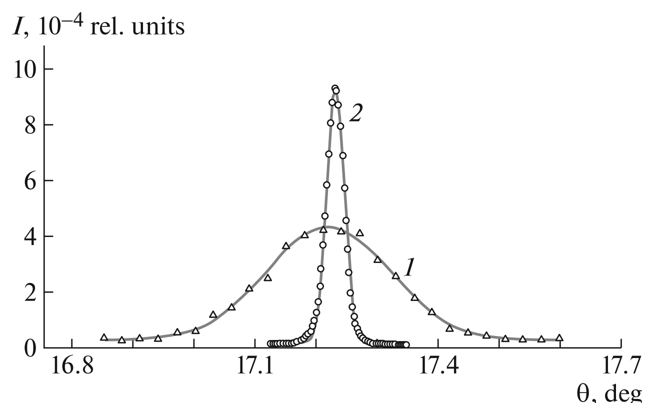

Fig. 5. Experimental rocking curves of a ZnO film from the (002) planes: (*1*) sample without a buffer AlN layer and (*2*) sample with an AlN layer. Symbols are experimental and the solid lines are approximations by Gaussian functions with an FWHM of (*1*) 0.237° and (*2*) 0.034°. The intensity normalized to the incident beam intensity is indicated. Curve *1* is multiplied by 350.

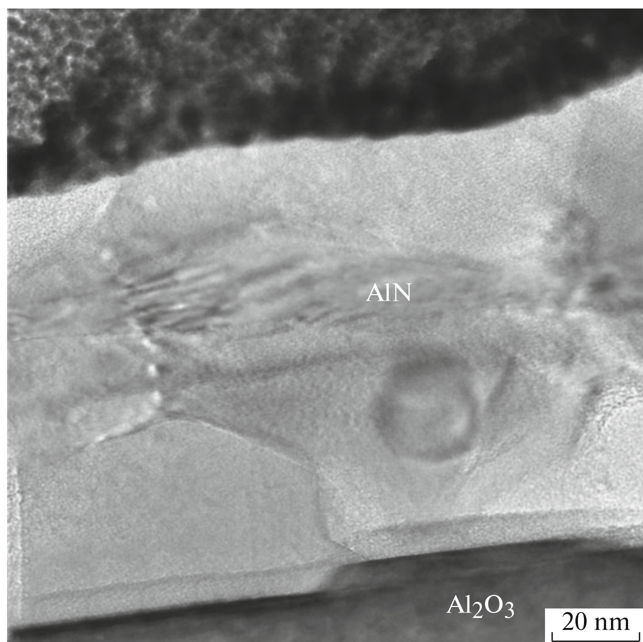

Fig. 6. Bright-field TEM image of a transverse cut of a sapphire substrate after thermochemical nitridation.

diffraction data show that thermochemical nitridation of the (0001) sapphire substrate surface improves the structural quality of epitaxial ZnO films significantly. Both compounds, ZnO and AlN, belong to the same (wurtzite) structural type and have similar unit-cell parameters (see the table), which ensures a better lattice matching at the interface.

In addition, it is well-known that, during the epitaxial growth of ZnO on Al_2O_3, the wurtzite and sapphire lattices rotate by 30° [4]: (0001) $[10\bar{1}0]$ZnO $\parallel$ (0001)$[11\bar{2}0]Al_2O_3$. In this case, the relation $a_{ZnO}\sqrt{3} > a_{AlN}\sqrt{3} > a_{Al_2O_3}$ is valid for both crystal layers and for the substrate (see the table). The intermediate AlN layer with intermediate lattice parameter *a* facilitates better lattice matching for the ZnO and AlN films by reducing stresses at the interface. The difference between the parameters of the AlN layer and sapphire is fairly large (13.4%), which may lead to the formation of differently oriented domains in the AlN layer during thermochemical nitridation (Fig. 6). The low concentration of domains and twins (Fig. 2) is apparently explained by the formation of the AlN film via the solid-state chemical reaction at nitrogen diffusion, with the replacement of oxygen on the sapphire substrate surface.

Concerning the further enhancement of the quality of epitxial ZnO films on sapphire substrates with nitridated surface, it primarily necessary to improve the structural quality of the AlN layers formed by thermochemical nitridation (in particular, reduce their surface roughness R_q). This can be done using the initial sapphire substrates with a super-smooth surface (R_q ~ 0.1 nm) and optimizing the gas mixture composition and temperature conditions via a decrease in the AlN layer thickness to 20–50 nm.

CONCLUSIONS

The morphology and surface structure of (0001) sapphire substrates subjected to thermochemical nitridation in a mixture of N_2, CO, and H_2 gases were studied by electron and probe microscopy and X-ray and electron diffraction. Sapphire substrates subjected to thermochemical nitridation were used for ZnO epitaxy. A comparative analysis of the heteroeptaxial ZnO/Al_2O_3 and $ZnO/AlN/Al_2O_3$ structures showed that the use of thermochemical nitridation of sapphire

substrates allows one to improve the quality of ZnO films.

ACKNOWLEDGMENTS

This study was carried out at the Center of Collective Use "Structural Diagnostics of Materials," Shubnikov Institute of Crystallography, Russian Academy of Sciences, and supported by the Ministry of Education and Science of the Russian Federation, project no. RFMEFI62114X0005; the Presidium of the Russian Academy of Sciences, Program of Basic Research no. 1 "Nanostructures: Physics, Chemistry, Biology, and Fundamentals of Technology"; the Russian Foundation for Basic Research, project nos.15-02-01197A, 14-22-01042 ofi_m, and state order no. 2560; and the Grant Council of the President of the Russian Federation (grant MK-4476.2014.2).

REFERENCES

1. K. K. Kim, J. H. Song, H. J. Jung, et al., J. Vac. Sci. Technol. A **18** (6), 2864 (2000).
2. M. Ying, X. Du, Z. Mei, et al., J. Phys. D **37**, 3058 (2004).
3. Y. Wang, S. Wang, S. Zhou, et al., Appl. Surf. Sci. **253**, 1745 (2006).
4. T. Trautnitz, R. Sorgenfrei, and M. Fiederle, J. Cryst. Growth **312**, 624 (2010).
5. A. V. Butashin, V. M. Kanevskii, A. E. Muslimov, et al., Crystallogr. Rep. **59** (3), 418 (2014).
6. V. P. Vlasov, A. V. Butashin, V. M. Kanevskii, et al., Crystallogr. Rep. **59** (3), 422 (2014).
7. E. N. Maslen, V. A. Streltsov, N. R. Streltsova, et al., Acta Crystallogr. B **29**, 973 (1993).
8. Yu. Goldberg, *Properties of Advanced Semiconductor Materials GaN, AlN, InN, BN, SiC, SiGe,* Ed. by M. E. Levinshtein et al. (Wiley, New York, 2001), p. 31.
9. H. Karzel, W. Potzel, M. Köfferlein, et al., Phys. Rev. B **53**, 11425 (1996).
10. S. V. Nizhankovskii, A. A. Krukhmalev, Ch. Sh. Kaltaev, et al., Phys. Solid State **54** (9), 1896 (2012).
11. S. A. Al'-Tkhuaeli, R. A. Rabadanov, A. M. Ismailov, et al., Vestn. DGU, Estestv. Nauki, No. **1**, 34 (2012).
12. M. V. Koval'chuk, P. A. Prosekov, M. A. Marchenkova, et al., Crystallogr. Rep. **59** (5), 679 (2014).
13. A. E. Blagov, A. L. Vasil'ev, A. S. Golubeva, et al., Crystallogr. Rep. **59** (3), 315 (2014).

Translated by E. Bondareva